International Journal of Applied Engineering Research
ISSN 0973-4562 Volume 20, Number 2 (2025) pp. 158-171

http://www.ripublication.com

Collision Avoidance Mechanisms using Artificial Potential Field for UAVs

Fadilah Abdul Azis[1*], Tan Jie Sim[1], Mariam Md Ghazaly[1], Noor Hazrin Hany Mohamad Hanif[2]

[1] *Motion Control Research Laboratory (MCon Lab), Fakulti Teknologi dan Kejuruteraan Elektrik (FTKE), Universiti Teknikal Malaysia Melaka, Melaka, Malaysia*

[2] *Kuliyyah of Engineering, International Islamic University Malaysia, Kuala Lumpur, Malaysia*

Abstract

This paper presents an enhanced implementation of the Artificial Potential Field (APF) algorithm for collision avoidance in Unmanned Aerial Vehicles (UAVs), targeting the challenges of autonomous navigation in dynamic environments. The APF algorithm, based on the combination of attractive and repulsive potential functions, is modeled and simulated in MATLAB to guide UAVs toward target destinations while avoiding obstacles. To evaluate algorithmic performance, three simulated scenarios were developed: (i) varying obstacle densities, (ii) extreme goal positioning, and (iii) external wind disturbances. The accuracy of UAV trajectory tracking was quantitatively assessed using Root Mean Square Error (RMSE). Experimental results show that the APF algorithm generates collision-free paths with increasing RMSE values under more complex conditions: 0.05921 in obstacle-free space, 0.06349 with three obstacles, and 0.08666 under wind disturbance, indicating a 36.5% accuracy degradation due to environmental perturbations. The novelty of this study lies in integrating wind dynamics into the APF model and the systematic use of RMSE as a performance metric across multiple environmental conditions. The developed simulation framework serves as a reproducible platform for benchmarking and future algorithmic extensions. This research demonstrates the APF algorithm's robustness and practical applicability while identifying limitations related to environmental adaptability and the need for parameter optimization in more complex flight conditions.

Keywords: Unmanned Aerial Vehicles (UAV); Collision avoidance; APF algorithm; Path planning; RMSE value.

Introduction

Unmanned Aerial Vehicles (UAVs), also referred to as drones, are a type of aircraft that can fly autonomously or be controlled remotely without the presence of a pilot [1]. A communication link, a ground control station, and unmanned aerial vehicles make up an Unmanned Aerial System. UAVs can provide cloud-free and high-resolution images. Hence, it is widely used in various applications such as delivery, monitoring, and mapping [2]–[4]. Nowadays, UAVs are equipped with cameras by merging radio-controlled aircraft with smartphone technology. To enable a UAV to fly autonomously, some important features become the main consideration of researchers when designing the UAV. Among these features, the computer algorithm is fundamental, as it enhances data processing and contributes to the overall performance of the UAV system. To stabilize the UAV flight, the algorithm can adjust the altitude and position of the UAV according to the condition by tracking the UAV's flight data [5]. Since UAVs always fly to in unpredictable conditions, various types of sensors such as ultrasonic sensors, cameras, and radar laser sensors are important for UAVs to detect the obstacles surrounding them [6]–[8]. The existing literature has identified four main categories that can lead to UAV accidents, which are human error, technical malfunctions, adverse weather conditions, and intentional tampering [8][9].

The obstacle avoidance system plays a significant role in reducing the probability of UAV accidents. This is because the obstacle avoidance system consists of algorithms and sensors to identify the presence and location of obstacles. Integrating specified algorithms on the UAV can aid the UAV in determining the best route to reach the goal without colliding with obstacles [10][11]. Autonomous flights always rely on algorithms to perform tasks such as object tracking and path planning [12][13]. If there are errors in these algorithms, it may cause the UAV to deviate from the planned route or fail to react to various conditions appropriately, which ultimately will cause a collision. In UAV systems, there are two types of computers: the flight controller and the mission computer. Some basic algorithms are pre-loaded into the flight controller's firmware to stabilize the UAV. Conversely, the algorithm related to special missions, such as path planning, is embedded in the mission computer. In this paper, the algorithm that will be investigated is related to collision avoidance and path planning. Recently, the integration of Artificial Potential Fields (APF) and consensus-based control algorithms has emerged as a prominent research area in cooperative formation control [14]. Notably, APF has established itself as a cornerstone technique for obstacle avoidance within such formations.

The APF algorithm was proposed by Khatib et al. in 1986, where particles represent UAVs and target points, while circles represent obstacles. The APF employs attractive forces in the direction of the goal and repulsive forces away from the obstacles; the UAVs move in the two-dimensional space according to the resultant force field. Although the APF algorithm is easy to implement and has been widely used in UAV trajectory planning because of its smooth trajectory generation, it has some problems, such as local minima, target unreachable, and trajectory oscillation in the narrow area [15]–[17]. Several modifications have been suggested to overcome these drawbacks. N. Wang et al. proposed an Improved APF (IAPF) integrated gain factors and repulsive potential field functions designed to handle both static and dynamic obstacles that improve UAV adaptability and flexibility in obstacle avoidance scenarios [18]. Seyyed et al. and Hu et al. presented modifications to enhance the obstacle avoidance and guarantee that the robot does not collide with the obstacles [19][20]. Chang et al. have proposed a new IAPF based on rotation vectors for path generation [21]. T. Manoni et al. have explored a combination of the virtual leader concept with the artificial potential field method for safe, collision-free multi-UAV formation control [22]. J. Huo et al. incorporated a segmented method for smooth navigation [23], Y. Xia et al. used structured approaches for adaptive control to ensure collision avoidance and enhance performance in dynamic environments [24], H. Sheng et al. [25] try to integrated of APF with a deformation factor to avoid local minima and last but not less the combination of repulsive APFs and rotation potential fields for navigation and collision avoidance was studied by A. Antony et al. [26]

Therefore, this paper proposes an enhanced implementation of the Artificial Potential Field (APF) algorithm to address the critical challenge of collision avoidance in Unmanned Aerial Vehicle (UAV) systems. Unlike prior studies that often focus on ideal or simplified conditions, this work systematically evaluates the performance of the APF algorithm under three distinct and practically relevant conditions: varying obstacle densities, extreme goal positioning, and external wind disturbances. The robustness and adaptability of the algorithm are quantitatively assessed using Root Mean Square Error (RMSE) values, enabling objective comparisons across scenarios of increasing environmental complexity.

The key contributions of this study are as follows: First, a comprehensive evaluation framework is developed to assess APF-based path planning across multiple operational stressors, providing a realistic benchmark for UAV navigation algorithms. Second, the inclusion of wind disturbance modelling—rarely addressed in existing literature—demonstrates the algorithm's responsiveness to environmental perturbations and highlights the significance of external forces on UAV trajectory accuracy. Third, applying RMSE as a quantitative metric enables a transparent assessment of navigational precision, with results indicating a 36.5% degradation in trajectory accuracy due to wind effects. Lastly, a MATLAB-based simulation platform has been developed to support reproducible experimentation and facilitate future research on APF-based or hybrid navigation strategies. These contributions collectively enhance the theoretical and practical understanding of APF-based UAV trajectory optimization and offer a valuable foundation for real-world deployment and further algorithmic development.

Method

The underlying concepts and mathematical equations associated with the APF algorithm are established to model the APF algorithm in MATLAB software. The APF algorithm is frequently used for path planning due to its safety and simplicity. A potential field is suitable for real-time applications. The APF algorithm involves two forces, attractive and repulsive, to avoid collision for the UAV. Obstacles generate a repulsive force, while the target location or goals generate an attractive force. The strength of the forces varies with the distance between the UAV and the obstacle or goal. Applying the APF algorithm, the obstacle repels the UAV while the goal attracts it. The resultant forces of the fields on the UAV are used to determine the direction of the UAV's motion. When applying the APF algorithm, the position vector of the UAV is considered as $q = (x, y)^T$. The APF function is represented by (1).

$$U(q) = U_{att}(q) + U_{rep}(q) \tag{1}$$

where $U(q)$ is the Artificial potential field exerted on UAV, $U_{att}(q)$ is the attractive field exerted by goal and $U_{rep}(q)$ is the repulsive field exerted by obstacle. According to Figure 1, an attractive force, F_{att} is directed towards the goal. The attractive force is generated from the goal to attract the UAV to move towards it. At the same time, there is a repulsive force, F_{rep} which is directed towards the opposite side of the obstacle. The repulsive force is generated by obstacles to repel the UAV. Force is the negative gradient of the potential field. The resultant force, F is the combination force of attractive force, F_{att} and repulsive force, F_{rep}. The direction of resultant force, F represents the direction of motion of the UAV.

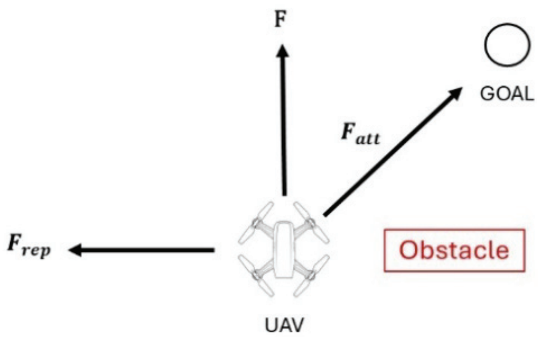

Figure 1. Resultant artificial force of potential function

The resultant force can be represented as in equation (2). The attractive field between the UAV and the goal is accumulated to attract the UAV to the goal area and can be calculated using equation (3). $F(q)$ is the resultant artificial force which moves the UAV, while $F_{att}(q)$ is the attractive force that is generated by the goal and $F_{rep}(q)$ is the repulsive force generated by the obstacle. Based on equation (3), k_a is the positive coefficient of gravity for APF, q and q_d are the current position vector of the UAV and the desired goal position vector, respectively. While ρ_{goal} is the Euclidean distance from the UAV's current position to the goal position. The attractive force applied to the UAV can be calculated as the negative gradient of the attractive potential field, as shown in (4).

$$F(q) = -\nabla U(q) = -\nabla U_{att}(q) - \nabla U_{rep}(q) = F_{att}(q) + F_{rep}(q \tag{2}$$

$$U_{att}(q) = \frac{1}{2} \times k_a \times \rho^2{}_{goal}(q) = \frac{1}{2} k_a \|q - q_d\|^2 \tag{3}$$

$$F_{att}(q) = -\nabla U_{att}(q) = -\frac{1}{2} k_a \rho^2{}_{goal}(q) = -k_a (q - q_d) \tag{4}$$

On the potential field, UAVs should be far from the obstacles. However, when the UAV is not close to the obstacles, its movement is unaffected by the obstacles in its path. Hence, the repulsion potential field, $U_{rep}(q)$, can be considered as 0. When the UAV is near the target, the repulsion potential field will gradually decrease. The repulsive potential field will be zero once the UAV successfully flies to the target. The repulsion potential field exerted on a UAV can be computed as (5). Based on (5), k_b is the repulsion gain coefficient, d is the distance between the UAV and the obstacle, and d_0 is the distance of the obstacle from the repulsive force field.

$$U_{rep}(q) = \begin{cases} \frac{1}{2} k_b \left({}^{1}/_{d(q)} - {}^{1}/_{d_0} \right)^2 , & d(q) \leq d_0 \\ 0 , & d(q) \geq d_0 \end{cases} \tag{5}$$

Consider the configuration of obstacles that is closest to the latest position of the UAV as $q_c = (x_c, y_c)$. The shortest distance between the UAV and obstacles is considered as $d = ||q - q_c||$ while the largest impact distance of the obstacle to the UAV is considered as d_0. When the UAV is close to the obstacle, a repulsive force is exerted on it. Conversely, there is no impact on the UAV when the distance between the UAV and the obstacle is greater than the largest impact distance, d_0. Hence, the repulsive force can be considered as 0.

The repulsive force can be calculated as follows:

$$F_{rep}(q) = \begin{cases} k_b \left({}^{1}/_{d(q)} \quad {}^{1}/_{d_0} \right) \left({}^{1}/_{d^2(q)} \right) \left({}^{q - q_c}/_{||q - q_c||} \right) , & d(q) \leq d_0 \\ 0 , & d(q) \geq d_0 \end{cases} \tag{6}$$

The repulsive force which exerted on the UAV are the combination of its cartesian components which are repulsion force in x and y directions, F_{repx}, F_{repy} respectively. The cartesian components of repulsion force, F_{repx} and F_{repy} can be calculated by applying (7) and (8).

$$F_{repx}(q) = \begin{cases} k_b \left({}^{1}/_{d(q)} - {}^{1}/_{d_0} \right) \left({}^{1}/_{d^2(q)} \right) \left({}^{x - x_c}/_{||q - q_c||} \right) , & d(q) \leq d_0 \\ 0 , & d(q) \geq d_0 \end{cases} \tag{7}$$

$$F_{repy}(q) = \begin{cases} k_b \left({}^{1}/_{d(q)} - {}^{1}/_{d_0} \right) \left({}^{1}/_{d^2(q)} \right) \left({}^{y - y_c}/_{||q - q_c||} \right) , & d(q) \leq d_0 \\ 0 , & d(q) \geq d_0 \end{cases} \tag{8}$$

If *n* number of obstacles are present in the environment, the artificial potential field, $U(q)$ and artificial force, $F(q)$ can be obtained as shown in (9) and (10), respectively.

$$U(q) = U_{att}(q) + \sum_{i=1}^{n} U_{rep}(q) \tag{9}$$

$$F(q) = F_{att}(q) + \sum_{i=1}^{n} F_{rep}(q) \tag{10}$$

To analyze the performance of the APF algorithm, three virtual environments: (a) number of obstacles, (b) extreme goal positioning, and (c) wind disturbance, which reflect the real-world conditions, are generated in MATLAB software. In each simulation condition, the path trajectory for the UAV to fly from the initial position (0,0) to the goal position (3.5, 3.5) is generated. In environment (a), the number of obstacles within the virtual environment varies from 0 to 3. For environment (b), the goal location of the UAV is shifted from (3.5, 3.5) to an extreme position at (100, 100). The simulation is executed under two scenarios: without obstacles and with three obstacles placed within the environment. In environment (c), the UAV takes off from (0,0) and navigates towards the goal position (3.5, 3.5) while encountering wind disturbances. The simulation is run under two conditions: with and without environmental obstacles. According to the simulation result, the Root Mean Square Error (RMSE) value is calculated to determine the accuracy of the UAV's positioning system as follows:

$$\text{RMSE} = \sqrt{\frac{1}{n} \sum_{i=1}^{n} (x_i - x_{gi})^2 + (y_i - y_{gi})^2} \tag{11}$$

A smaller RMSE value indicates that the model's predictions are closer to the actual data, while a larger RMSE suggests greater error in the predictions.

Results and Discussion

This section presents the results of three simulations designed to evaluate the performance of the Artificial Potential Field (APF) algorithm in guiding the UAV through diverse environments. The simulations investigate scenarios with varying numbers of obstacles, extreme goal positions and wind disturbances. The effectiveness of the APF algorithm in generating collision-free trajectories towards designated goals is assessed by analyzing UAV position data collected during each simulation.

3.1. Number of Obstacles

The algorithm for generating Unmanned Aerial Vehicles (UAVs) trajectories in environments with different levels of obstacle complexity will be evaluated. Figure 2 depicts the trajectory of the UAV with varying numbers of obstacles, namely 0, 1, 2, and 3. The obstacles consist of varying-sized rectangular boxes positioned from the starting point to the target address. The UAV was initially positioned at coordinates (0,0) and its target position at coordinates (3.5,3.5). The position of the UAV is consistently updated and documented in a table to assess the accuracy of the positioning system using the RMSE value. The simulation results shown in Figure 2 start with a UAV trajectory with no obstacle, as in Figure 2(a), to a trajectory with only one, two, and three obstacles, as in Figure 2(b), Figure 2(c), and Figure 2(d), respectively. These demonstrate that the APF algorithm excels in producing collision-free trajectories for UAVs as they navigate towards specified target locations in environments with varying obstacles.

The accomplishment can be attributed to the combination of attractive and repulsive forces. An attractive force propels the UAV towards its intended destination, while a repulsive force steers it away from obstacles to prevent collisions. The deviation of the UAV from the goal position can be determined through the RMSE value shown in Table 1. A lower RMSE value shown by the trajectory without an obstacle, i.e., 0.05921, indicated that the actual position of the UAV is close to the goal position. A higher RMSE value shown by the trajectory with three (3) obstacles, i.e., 0.06349, suggests a discrepancy between the UAV's position and goal position. As the number of obstacles increases, the RMSE value rises. A higher number of obstacles generates a more repulsive force towards the UAV. Hence, the UAV experiences greater deviation from its original path to avoid collision with obstacles. The deviations lead to a higher value of RMSE.

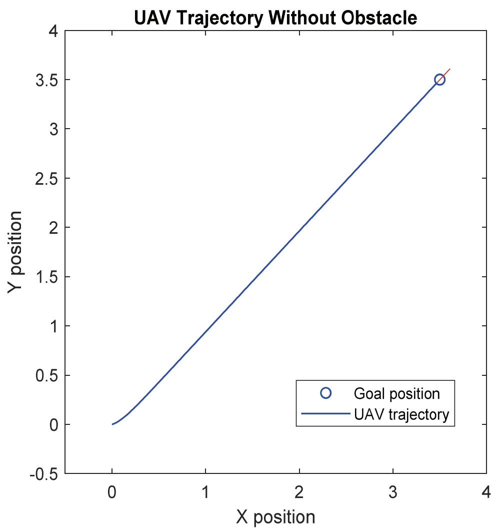

(a)

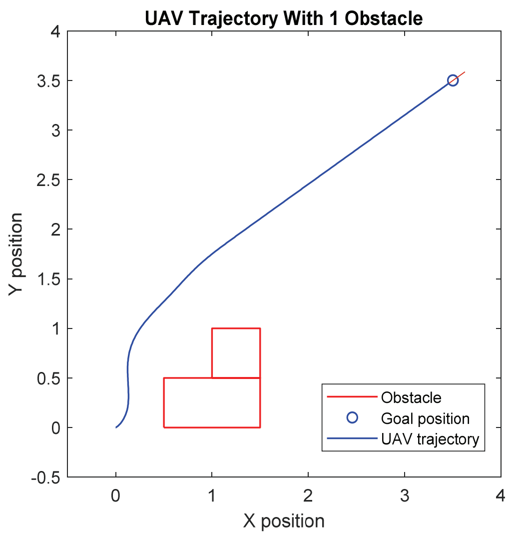

(b)

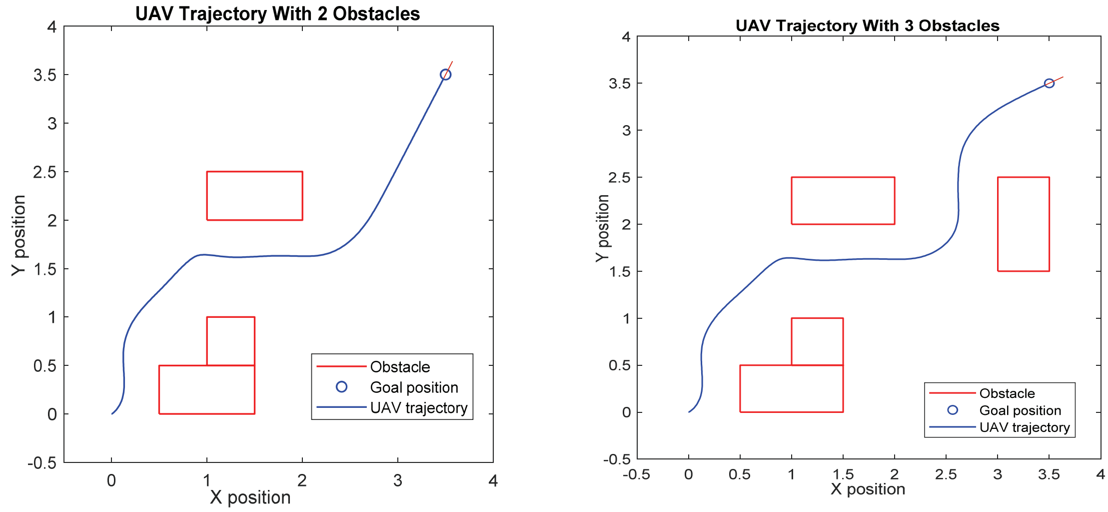

(c) (d)

Figure 2. UAV Trajectory; (a) without obstacle, (b) 1 obstacle, (c) 2 obstacles, and (d) 3 obstacles

Table 1. RMSE value for different numbers of obstacles

Number of Obstacles	RMSE
Without Obstacle	0.05921
1 Obstacle	0.06330
2 Obstacles	0.05874
3 Obstacles	0.06349

3.2. Extreme Goal Position

The UAV trajectory generation for extreme goal positions is simulated under two conditions: obstacle-free and with three obstacles within the environment, as illustrated in Figure 3. The initial position of the UAV is located at coordinate (0, 0) while the goal position is located at coordinate (100,100). The UAV's position is continuously updated for RMSE-based accuracy assessment. In obstacle-free environments, the APF algorithm guides the UAV directly towards the extreme position of the goal using a strong attractive force, as shown in Figure 3(a). As the UAV approaches the goal, the attractive force acting on the UAV decreases. Hence, a UAV can stop precisely at the goal position. In an environment with three obstacles, as shown in Figure 3(b), the UAV must consider the total repulsion potential field from the three obstacles to reach the goal position. Simultaneously, an attractive force attracts the UAV to move towards the direction of the goal.

Finally, the UAV reached the goal position without colliding with the obstacles. A long path is necessary for the UAV to reach the goal in an extreme location. Small deviations accumulate over time as the UAV navigates over a long distance. Therefore, the RMSE value is elevated as shown in Table 2. The RMSE value of an environment without obstacles, i.e., 0.06351, is greater than that of an environment with obstacles, i.e., 0.06338. The APF algorithm's fundamental principle is to produce an optimal path by achieving a balance between the attractive and repulsive forces. In an environment without obstacles, the UAV can exceed its intended destination. Thus, it may result in an increased RMSE value. However, the accuracy of both UAV trajectories is still good as their RMSE values stay lower at 0.06.

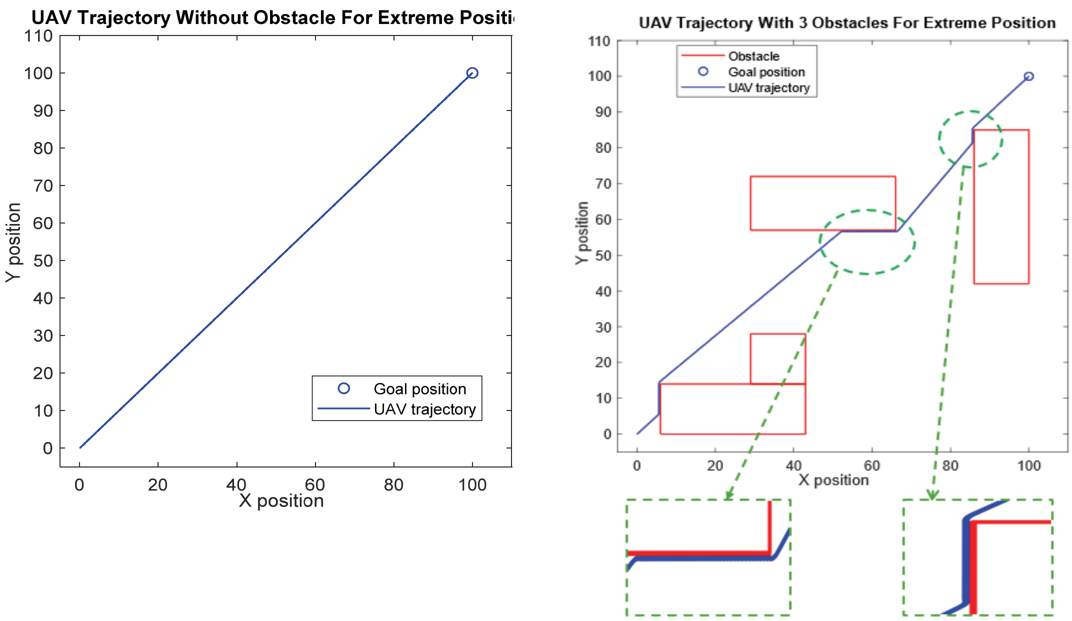

(a) (b)

Figure 3. UAV trajectory analysis using APF algorithm for extreme position; (a) Without obstacle, and (b) 3 obstacles

Table 2. RMSE value for the extreme position of the goal

Number of Obstacles	RMSE
Without Obstacle	0.06351
3 Obstacles	0.06338

3.3. Wind Disturbance

The introduction of wind disturbances presents a new challenge for UAV navigation. In this research, the simulated UAV trajectories within an environment that are subjected to wind disturbances have two distinct scenarios, i.e., (i) without obstacles and (ii) with three obstacles. In this case, the wind effect is added to the simulated environment. The wind effect is presumed to continuously blow from the south to the north. The UAV must navigate from the initial position at coordinate (0, 0) to a designated goal at coordinate (3.5, 3.5) while accommodating these wind disturbances. The UAV's positional data is continuously collected and rigorously evaluated using the Root Mean Square Error (RMSE) metric to assess the positioning system's accuracy.

From Figure 4(a), the UAV is attracted to the direction of the goal due to the presence of an attractive force with the additional wind effect. The APF algorithm detects deviation and increases the attractive force towards the goal to counteract the wind. In Figure 4(b), the presence of obstacles and wind effects significantly complicates UAV navigation. Compared to wind-free scenarios, the UAV's trajectory diverges considerably due to wind disturbances. It is important to note that the APF algorithm identified a potential collision risk with the second obstacle if the UAV continued along its original path between the first and second obstacles during wind disturbances. The distance between the UAV and the obstacle reaches the maximum distance of the obstacle repulsive force field due to the combined effect of wind and obstacle. Consequently, a more potent repulsive force is produced to deflect the UAV from the obstructions. As a result, the trajectory of the UAV was substantially altered to prevent this collision.

Wind disturbances have a substantial effect on the positioning accuracy of the UAV, as seen by the higher RMSE values shown in Table 3, namely 0.086, compared to wind-free situations, as shown in Table 1 and Table 2, namely 0.063. This data indicates a 36.5% expansion in the impact of wind disturbances on the accuracy of UAV trajectories. Wind disrupts the UAV's planned trajectory, causing deviations and hindering stable flight. To mitigate these wind effects, the APF algorithm dynamically adjusts the attractive force acting on the UAV. The APF algorithm steers the UAV back towards its intended path by increasing the attractive force in response to wind-induced deviations. This compensatory mechanism helps the UAV reach the goal position while navigating the challenges of wind disturbances.

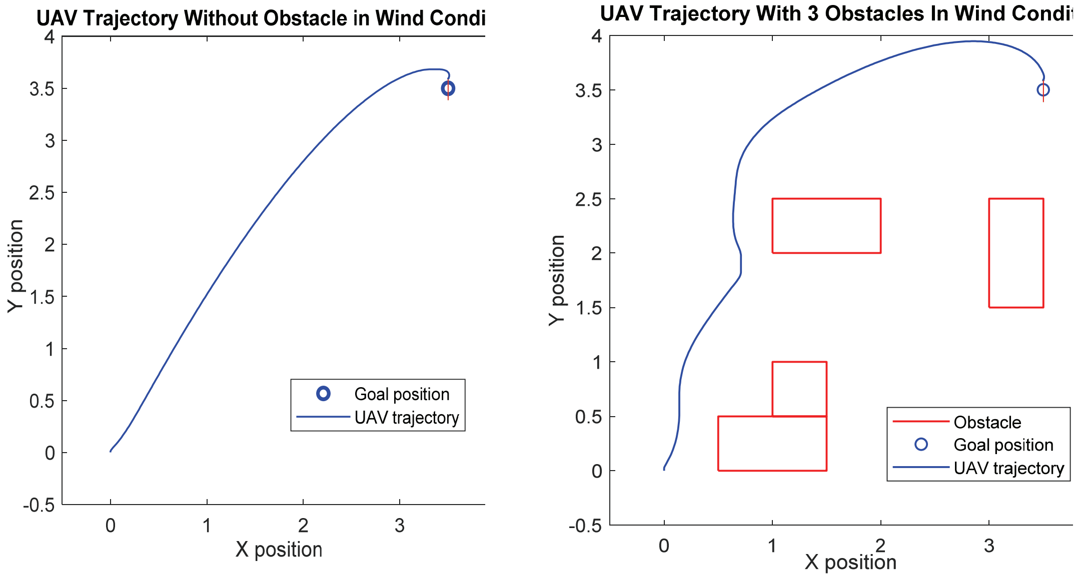

(a) (b)

Figure 4. UAV trajectory with wind effect; (a) Without obstacle, (b) 3 obstacles.

Table 3. RMSE value for wind disturbances

Number of Obstacles	RMSE
Without Obstacle	0.08666
3 Obstacles	0.08670

Conclusion

This study has demonstrated that the Artificial Potential Field (APF) algorithm is a practical and effective method for collision avoidance in Unmanned Aerial Vehicle (UAV) navigation, particularly when confronted with varying environmental complexities. The evidence supporting this conclusion is grounded in a series of controlled MATLAB-based simulations conducted under three distinct operational scenarios: increasing obstacle densities, extreme goal positioning, and environmental wind disturbances. In each scenario, the trajectory of the UAV was quantitatively evaluated using Root Mean Square Error (RMSE), which served as the primary metric for assessing positional accuracy and path fidelity. The resulting data revealed a direct correlation between environmental complexity and navigational deviation. Specifically, RMSE increased from 0.05921 in an obstacle-free environment to 0.06349 in the presence of three obstacles, while extreme goal positioning and wind disturbances further elevated RMSE to 0.06351 and 0.08666, respectively. These results constitute rigorous, numerical evidence of the strengths and limitations of the APF algorithm.

The significance of these findings lies in their implications for both the academic field and the broader UAV development community. From a research standpoint, the study provides a reproducible simulation framework. It introduces a quantitative benchmarking method that can be used to evaluate and compare future collision avoidance algorithms under realistic constraints. For practitioners, the results underscore the robustness of the APF algorithm in generating collision-free paths even in the presence of adverse conditions, while also identifying wind disturbances as a dominant factor affecting trajectory accuracy. This highlights the need for adaptive tuning or hybrid algorithmic strategies in future implementations. Overall, the findings contribute to the advancement of autonomous UAV navigation by establishing a performance baseline and identifying critical areas for improvement, thereby informing both theoretical development and real-world system design.

Acknowledgements
The authors wish to extend their utmost appreciation to the Centre for Research and Innovation Management (CRIM) and Universiti Teknikal Malaysia Melaka (UTeM) for the support of facilities and funds provided during the research.

References

[1] A. T. Oyelami, A. S. Akinade, and K. C. Obianefo, "Development of a real-time framework for farm monitoring using drone technology," IAES Int. J. Robot. Autom., vol. 9, no. 4, p. 244, 2020.

[2] X. Deng, M. Guan, Y. Ma, X. Yang, and T. Xiang, "Vehicle-Assisted UAV Delivery Scheme Considering Energy Consumption for Instant Delivery," Sensors, vol. 22, no. 5, 2022.

[3] H. C. Park, T. S. N. Rachmawati, and S. Kim, "UAV-Based High-Rise Buildings Earthwork Monitoring-A Case Study," Sustain., vol. 14, no. 16, 2022.

[4] V. Šafář et al., "The use of UAV in cadastral mapping of the Czech Republic," ISPRS Int. J. Geo-Information, vol. 10, no. 6, 2021.

[5] E. E. Papadopoulou, C. Vasilakos, N. Zouros, and N. Soulakellis, "DEM-based UAV flight planning for 3D mapping of geosites: The case of Olympus tectonic window, Lesvos, Greece," ISPRS Int. J. Geo-Information, vol. 10, no. 8, 2021.

[6] J. Upadhyay, A. Rawat, and D. Deb, "Multiple drone navigation and formation using selective target tracking-based computer vision," Electron., vol. 10, no. 17, 2021.

[7] C. Weber, J. von Eichel-Streiber, J. Rodrigo-Comino, J. Altenburg, and T. Udelhoven, "Automotive radar in a UAV to assess earth surface processes and land responses," Sensors (Switzerland), vol. 20, no. 16, pp. 1–19, 2020,

[8] Y. Rong, R. Gutierrez, K. V. Mishra, and D. W. Bliss, "Noncontact Vital Sign Detection with UAV-Borne Radars: An Overview of Recent Advances," IEEE Veh. Technol. Mag., vol. 16, no. 3, pp. 118–128, 2021,

[9] Ben Grindley, Katie Phillips, Katie J. Parnell, Tom Cherrett, James Scanlan, Katherine L. Plant, "Over a decade of UAV incidents: A human factors analysis of causal factors," Applied Ergonomics, Volume 121,2024, 104355

[10] Z. Wu, J. Dai, B. Jiang, and H. R. Karimi, "Robot path planning based on artificial potential field with deterministic annealing," ISA Trans., vol. 138, pp. 74–87, 2023.
[11] L. Van Nguyen, N. M. Kwok, and Q. P. Ha, "Fermat-Weber location particle swarm optimization for cooperative path planning of unmanned aerial vehicles," Appl. Soft Comput., vol.. 167, no. PA, p. 112269, 2024,
[12] M. Bolognini and L. Fagiano, "Lidar-based navigation of tethered drone formations in an unknown environment," IFAC-PapersOnLine, vol. 53, no. 2, pp. 9426–9431, 2020.
[13] F. A. de A. Andrade et al., "Autonomous unmanned aerial vehicles in search and rescue missions using real-time cooperative model predictive control," Sensors (Switzerland), vol. 19, no. 19, 2019.
[14] J. Alonso-Mora, E. Montijano, T. Nägeli, O. Hilliges, M. Schwager, and D. Rus, "Distributed multi-robot formation control in dynamic environments," Auton. Robots, vol. 43, no. 5, pp. 1079–1100, 2019.
[15] F. Arambula Cosío and M. A. Padilla Castañeda, "Autonomous robot navigation using adaptive potential fields," Math. Comput. Model, vol. 40, no. 9–10, pp. 1141–1156, 2004.
[16] A. N. A. Rafai, N. Adzhar, and N. I. Jaini, "A Review on Path Planning and Obstacle Avoidance Algorithms for Autonomous Mobile Robots," J. Robot., vol. 2022, 2022.
[17] F. Kong, W. Xu, Y. Cai, and F. Zhang, "Avoiding Dynamic Small Obstacles with Onboard Sensing and Computation on Aerial Robots," IEEE Robot. Autom. Lett., vol. 6, no. 4, pp. 7869–7876, 2021.
[18] N. Wang, J. Dai, and J. Ying, "UAV Formation Obstacle Avoidance Control Algorithm Based on Improved Artificial Potential Field and Consensus," Int. J. Aeronaut. Sp. Sci., vol. 22, no. 6, pp. 1413–1427, 2021.
[19] S. Mohammad, H. Rostami, A. K. Sangaiah, and J. Wang, "Obstacle avoidance of mobile robots using modified potential field algorithm," Eurasip J. Wirel. Commun. Netw., vol. 2019, no. 1, pp. 1–19, 2019.
[20] J. W. Hu, M. Wang, C. H. Zhao, Q. Pan, and C. Du, "Formation control and collision avoidance for multi-UAV systems based on Voronoi partition," Sci. China Technol. Sci., vol. 63, no. 1, pp. 65–72, 2020.
[21] K. Chang, D. Ma, X. Han, N. Liu, and P. Zhao, "Lyapunov vector-based formation tracking control for unmanned aerial vehicles with obstacle/collision avoidance," Trans. Inst. Meas. Control, vol. 42, no. 5, pp. 942–950, 2020.
[22] T. Manoni, D. Albani, J. Horyna, P. Petracek, M. Saska, and E. Ferrante, "Adaptive arbitration of aerial swarm interactions through a Gaussian kernel for coherent group motion," Front. Robot. AI, vol.. 9, no. December, pp. 1–14, 2022.
[23] J. Huo, S. L. Zenkevich, A. V. Nazarova, and M. Zhai, "Path planning based on map matching in UAV/UGV collaboration system," Int. J. Intell. Unmanned Syst., vol. 9, no. 2, pp. 81–95, 2019.
[24] Y. Xia, X. Shao, Z. Mei, and W. Zhang, "Performance-Designated Reinforcement Learning Enclosing Control for UAVs With Collision-Free

Capability," IEEE Trans. Intell. Transp. Syst., vol. 25, no. 9, pp. 12644–12656, 2024.

[25] H. Sheng et al., "New multi-UAV formation keeping method based on improved artificial potential field," Chinese J. Aeronaut., vol. 36, no. 11, pp. 249–270, 2023.

[26] A. Antony, S. R. Kumar, and D. Mukherjee, "Artificial Potential Fields based Formation Control for Fixed Wing UAVs with Obstacle Avoidance," IFAC-PapersOnLine, vol. 57, pp. 54–59, 2024